Subdiffusion as a model of transport through the nuclear pore complex

Debarati Chatterjee and Binny J. Cherayil

Citation: The Journal of Chemical Physics **135**, 155101 (2011); doi: 10.1063/1.3651100
View online: http://dx.doi.org/10.1063/1.3651100
View Table of Contents: http://scitation.aip.org/content/aip/journal/jcp/135/15?ver=pdfcov
Published by the AIP Publishing

Subdiffusion as a model of transport through the nuclear pore complex

Debarati Chatterjee and Binny J. Cherayil[a)]
Department of Inorganic and Physical Chemistry, Indian Institute of Science, Bangalore 560012, India

(Received 28 June 2011; accepted 22 September 2011; published online 19 October 2011)

Cargo transport through the nuclear pore complex continues to be a subject of considerable interest to experimentalists and theorists alike. Several recent studies have revealed details of the process that have still to be fully understood, among them the apparent nonlinearity between cargo size and the pore crossing time, the skewed, asymmetric nature of the distribution of such crossing times, and the non-exponentiality in the decay profile of the dynamic autocorrelation function of cargo positions. In this paper, we show that a model of pore transport based on subdiffusive particle motion is in qualitative agreement with many of these observations. The model corresponds to a process of stochastic binding and release of the particle as it moves through the channel. It suggests that the phenylalanine-glycine repeat units that form an entangled polymer mesh across the channel may be involved in translocation, since these units have the potential to intermittently bind to hydrophobic receptor sites on the transporter protein. © *2011 American Institute of Physics*. [doi:10.1063/1.3651100]

I. INTRODUCTION

In living cells, the selective transport of macromolecules across the barrier separating the cytoplasm from the nucleus is mediated by an assembly of transmembrane proteins (called the nuclear pore complex or NPC) that nicely illustrates Nature's precision engineering.[1] But we still do not fully understand how this roughly 90 nm long hour-glass structure that is about 70 nm wide at its ends and 45 nm at its waist discriminates between different molecules, letting some go through and blocking out others. We do know that molecules with masses of 20–40 kDa and sizes less than about 9 nm get across the channel by simple diffusion, and that molecules with masses greater than 40 kDa and sizes of about 32–36 nm are either turned back or are actively helped across by a mechanism that seems to be tied up with the hydrophobic protein mesh that lines the pore walls and intrudes into its lumen.[2]

The role of cargo size is, in fact, one aspect of transport through the channel that remains somewhat obscure. For instance, simulations by Moussavi-Baygi *et al.*[3] and Mincer and Simon[4] have shown, using coarse-grained models of the NPC that incorporate a range of structural features with varying degrees of fidelity to the actual architecture of the pore, that above a certain threshold value the mean first passage time (MFPT) to cross the channel varies *nonlinearly* with the size of the cargo. Had simple diffusion been the underlying mechanism of transport, however (and assuming negligible confinement effects), one would have expected the variation to be linear. Other aspects of the transport process do not seem to conform to a simple diffusion model either. In particular, recent single-particle tracking experiments by Lowe *et al.*[5] have found that the mean square displacement (MSD) of cargo particles is a *sublinear* function of the time. The observation of a wide distribution of dwell times in these experiments as well as in the most recent simulations of Moussavi-Baygi *et al.*[6] also seems to militate against a mechanism based on simple diffusion. On the other hand, Hermann *et al.*[7] have shown from experiments on the fluorescence intensity correlation function of labeled transporter proteins passing through free-standing NPCs that simple diffusion can account for the time dependence of fluctuations in cargo positions. That simple diffusion seems to explain some findings but not others may indicate that the actual transport mechanism is more general.

In this paper, we should like to suggest that, in fact, the mechanism involves subdiffusion. As is well-known subdiffusive motion is characterized by mean square particle displacements that vary sublinearly with time.[8] It typically occurs in viscoelastic media, such as polymer solutions, where thermal fluctuations tend to be correlated over long periods of time, and it can be explained on the basis of a continuous time random walk model (CTRW) in which the waiting time between successive steps in the walk is governed by a power law distribution.[9] Physically, subdiffusion may be visualized in terms of the motion of a diffusing particle that is trapped every now and then, and then freed after a random interval that is drawn from a distribution of algebraically decaying times. Transporter proteins do have sites that can bind to the hydrophobic-rich regions of the phenylalanine-glycine residues in the polymer brush that straddles the pore,[10] so stochastic binding and release is a plausible scenario for how the proteins are ferried across the channel.

In the formalism of CTRWs with power law waiting times, the probability density function of particle positions at time t is governed by an equation that contains fractional time derivatives[9] and that is a generalization of the ordinary Smoluchowski equation. If the NPC is idealized as a hollow cylinder (as was recently done by Licata and Grill[11] in a model based on intermittent attachment to the *walls* of a cylinder), the solution of this generalized Smoluchowski equation under appropriate boundary conditions can, in principle, be used to calculate various statistical properties of the transport process. But if the MFPT is calculated in this way, using CTRWs, the result can be shown to diverge.[12] So the

[a)]Author to whom correspondence should be addressed. Electronic mail: cherayil@ipc.iisc.ernet.in.

CTRW approach does not really work as a model of transport through the NPC, even though the physics that underlies it—random motion interrupted by random waiting times, leading to subdiffusion—seems reasonable.

But there are other routes to subdiffusion. In particular, it can be produced when the random forces that drive particle motion originate in fractional Gaussian noise[13] (fGn), and are therefore power law correlated in time. When this is the case, the probability density function for particle positions evolves by another variant of the Smoluchowski equation, one in which the diffusion coefficient is time dependent.[14] In a cylindrical domain, this generalized Smoluchowski equation, like the CTRW approach, should be able to serve as a model of transport through the NPC, since it is also built around the notion of subdiffusion. This is a possibility we explore in this paper, following the general methods discussed by Licata and Grill in Ref. 11 and Chaudhury and Cherayil in Ref. 15. In particular, we use the model to calculate the MSD, the MFPT, the MFPT distribution, and the fluorescence intensity correlation function. From our results, we draw some general conclusions about transport through the NPC.

Section II sets down the generalized Langevin equation (in Cartesian coordinates) that forms the basis of our theoretical analysis. This equation is used to derive expressions for the MSD and the equation for the evolution of the probability density of particle positions, a Smoluchowski equation. After a transformation to cylindrical coordinates, the Smoluchowski equation is solved under suitable boundary conditions in Sec. III, and then used to determine, first, the MFPT to cross the cylinder and the MFPT distribution, and next, in Sec. IV, the dynamic autocorrelation function of fluorescence intensity fluctuations. We discuss these results in Sec. V.

II. THEORETICAL FORMALISM

In general, the dynamics of a particle moving through a fluid under the action of random thermal forces can be described by a simple Langevin equation. If the fluid is viscoelastic, however, as we assume is the case for the medium within the NPC, the dynamics are better described by the following generalized Langevin equation (GLE)[16]

$$m\ddot{x}_i(t) = -\zeta\int_0^t dt' K(t-t')\dot{x}_i(t') + \theta_i(t), i = 1, 2, 3, \quad (1)$$

where $x_i(t)$ is the ith component (in Cartesian coordinates) of the position of a particle at time t, m is its mass, $\theta_i(t)$ is the ith component of the random force at time t, ζ is a generalized friction coefficient, and $K(t-t')$ is a memory function. The random force and the memory function are related by a fluctuation-dissipation theorem: $\langle\theta_i(t)\theta_j(t')\rangle = \zeta k_B T K(|t-t'|)\delta_{ij}$, with k_B the Boltzmann constant and T the absolute temperature. In the present calculations, we take the random force to correspond to fGn, which means that for $t > 0$, $K(t) = 2H(2H-1)|t|^{2H-2}$, where H, the so-called Hurst index, is a real number between 1/2 and 1 that provides a measure of how strongly successive random forces are correlated with each other in time. The larger the H, the greater the correlation.

The mean square displacement of a particle that obeys Eq. (1) has been determined earlier in one dimension;[15] in three dimensions, the corresponding expression (GLE) is

$$\langle\delta\mathbf{x}^2(t)\rangle = 6\int_0^t dt' D(t'), \quad (2a)$$

where $\delta\mathbf{x}(t) = \mathbf{x}(t) - \mathbf{x}(0)$ and $D(t)$ are the effective diffusion coefficient alluded to in the Introduction, which can be shown[15] to have the explicit form $D(t) = (k_BT/m)tE_{2H,2}[-(t/\tau)^{2H}]$. Here, $E_{a,b}(-z) \equiv \sum_{k=0}^{\infty}(-z)^k/\Gamma(ak+b)$ is the generalized Mittag-Leffler function, $\Gamma(x)$ is the gamma function, and $\tau \equiv (m/\zeta\Gamma(2H+1))^{1/2H}$. The integral in Eq. (2a) can actually be evaluated in closed form,[15] after which $\langle\delta\mathbf{x}^2(t)\rangle$ is reduced to

$$\langle(\delta\mathbf{x}(t)^2\rangle = \frac{6k_BT}{m}t^2E_{2H,3}[-(t/\tau)^{2H}], \quad (2b)$$

or in dimensionless form to

$$\langle(\delta\mathbf{x}(t)^2\rangle/6l^2 = \bar{t}^2E_{2H,3}[-\bar{t}^{2H}], \quad (2c)$$

where $l \equiv \sqrt{k_BT\tau^2/m}$ and $\bar{t} \equiv t/\tau$. For large values of its argument, the Mittag-Leffler function behaves asymptotically as[17] $E_{a,b}(-z) \sim 1/z\Gamma(b-a)$, so in the long time limit, that is, when $t/\tau \gg 1$, $\langle\delta\mathbf{x}(t)^2\rangle \sim t^{2-2H}$. In other words, when $H \neq 1/2$, the motion of the particle is subdiffusive, which is the behavior we believe is characteristic of a transport mechanism based on stochastic binding and release. (When $H = 1/2$, the motion is, of course, diffusive, and $D(t) \to k_BT/\zeta = D_0$.)

For the purposes of calculating a MFPT, or a first passage time distribution, or a time correlation function, what is needed is not the equation of motion of the particle itself, but the equation for the evolution of its probability density function, $P(\mathbf{x}, t)$, defined as $P(\mathbf{x}, t) = \langle\delta(\mathbf{x} - \mathbf{x}(t)\rangle$, where the angular brackets denote an average over different realizations of the noise, and of the initial equilibrium state of the system. The conversion of Eq. (1) to an equivalent equation for $P(\mathbf{x}, t)$ is a fairly standard exercise in functional calculus[18] and has been worked out earlier.[15] We therefore report only the final result, which is

$$\frac{\partial P(\mathbf{x}, t)}{\partial t} = D(t)\nabla_{\mathbf{x}}^2 P(\mathbf{x}, t), \quad (3)$$

with $D(t)$ defined above. Equation (3) must be solved subject to boundary and initial conditions appropriate to the cylindrical geometry we have assumed for the NPC channel. Because of the radial symmetry of the problem, it proves convenient to seek the solution in cylindrical coordinates (r, φ, z) rather than Cartesian coordinates (x, y, z). The relation between the two is defined by

$$x = r\cos\varphi, \quad y = r\sin\varphi, \quad z = z, \quad (4)$$

where $0 \le r \le \infty$, $0 \le \varphi \le 2\pi$, and $0 \le z \le \infty$. In cylindrical coordinates, Eq. (3) is

$$\left[\frac{\partial}{\partial t} - D(t)\left\{\frac{\partial^2}{\partial r^2} + \frac{1}{r}\frac{\partial}{\partial r} + \frac{1}{r^2}\frac{\partial^2}{\partial\varphi^2} + \frac{\partial^2}{\partial z^2}\right\}\right]P(r, \varphi, z, t) = 0. \quad (5)$$

For the calculation of the MFPT, we impose the following boundary conditions on the solution of Eq. (5):

$$\left.\frac{\partial P}{\partial z}\right|_{z=0} = 0, \quad \left.\frac{\partial P}{\partial r}\right|_{r=R} = 0, \quad \text{and } P|_{z=L} = 0 \tag{6a}$$

Here L is the length of the cylinder and R is its radius. The first condition in Eq. (6a) corresponds to reflection at the plane $z = 0$, the second to reflection at the cylinder walls (located at $r = R$), and the last to absorption at the plane $z = L$. (In the calculations of Licata and Grill,[11] the second of the conditions in Eq. (6a) was replaced by the absorption condition $P(r = R) = 0$ in order to model a cylinder with sticky walls.) Equation (6a) is supplemented by the initial condition

$$P(r, \varphi, z, 0) = \frac{1}{r}\delta(r - r_0)\delta(\varphi - \varphi_0)\delta(z - z_0). \tag{6b}$$

For the calculation of the intensity autocorrelation function, the boundary conditions are

$$\left.\frac{\partial P}{\partial z}\right|_{z=0} = 0, \quad \left.\frac{\partial P}{\partial r}\right|_{r=R} = 0, \quad \text{and} \left.\frac{\partial P}{\partial z}\right|_{z=L} = 0, \tag{7}$$

the initial condition remaining the same. The reflecting boundary condition at $z = L$ is introduced to ensure that there is an equilibrium distribution of particles at long times.

III. THE MEAN FIRST PASSAGE TIME AND ITS DISTRIBUTION

To solve Eq. (5) with the boundary conditions of Eq. (6a) and the initial condition of Eq. (6b), we first expand $P(r, \varphi, z, t)$ in a complete set of eigenfunctions:

$$P(r,\varphi,z,t) = \sum_{m_1}\sum_{n_1}\sum_{k_1} A_{m_1n_1k_1} e^{im_1\varphi} J_{m_1}(y_{m_1n_1} r/R) \times \cos[(2k_1+1)\pi z/2L] \exp\left[-\lambda_{m_1n_1k_1}\int_0^t dt' D(t')\right], \tag{8}$$

where $J_{m_1}(x)$ is the Bessel function of order m_1, $y_{m_1n_1}$ is the n_1th zero of $J'_{m_1}(x)$, i.e., $J'_{m_1}(y_{m_1n_1}) = 0$, the prime denoting differentiation, and $A_{m_1n_1k_1}$ and $\lambda_{m_1n_1k_1}$ are unknown constants to be determined. The eigenvalues $\lambda_{m_1n_1k_1}$ are found by substituting Eq. (8) into Eq. (5), and using the relation $J_{\nu''}(x) + (1/x)J_{\nu'}(x) + (1 - \nu^2/x^2)J_\nu(x) = 0$ (Ref. 19) to simplify the expression; the result is

$$\lambda_{m_1n_1k_1} = \left(\frac{y_{m_1n_1}}{R}\right)^2 + \left(\frac{(2k_1+1)\pi}{2L}\right)^2. \tag{9}$$

The parameters $A_{m_1n_1k_1}$ are found from the initial condition applied to Eq. (8), which yields

$$\frac{1}{r}\delta(r - r_0)\delta(\varphi - \varphi_0)\delta(z - z_0) = \sum_{m_1}\sum_{n_1}\sum_{k_1} A_{m_1n_1k_1} e^{im_1\varphi} J_{m_1}(y_{m_1n_1} r/R) \times \cos[(2k_1+1)\pi z/2L]. \tag{10}$$

This expression is multiplied by $re^{-im_2\varphi} J_{m_2}(y_{m_2n_2} r/R) \cos[(2k_2+1)\pi z/2L]$ and then integrated over φ from 0 to 2π, over r from 0 to R, and over z from 0 to L. The integrals over φ and z on the right hand side of the equation are elementary; they produce $2\pi\delta_{m_1m_2}$ and $L\delta_{k_1k_2}/2$, respectively. The integral over r, subject to the condition $J'_{m_2}(y_{m_2n_2}) = 0$, is given by

$$\int_0^R dr r J_{m_2}(y_{m_2n_1} r/R) J_{m_2}(y_{m_2n_2} r/R) = \frac{R^2}{2}\delta_{n_1n_2}\left(1 - \frac{m_2^2}{y_{m_2n_2}^2}\right) J_{m_2}^2(y_{m_2n_2}). \tag{11}$$

From these results, one easily finds $A_{m_1n_1k_1}$, and after substituting it back into the expression for $P(r, \varphi, z, t)$, one finally obtains

$$P(r, \varphi, z, t|r_0, \varphi_0, z_0) = \frac{2}{\pi L R^2}\sum_{mnk}\frac{y_{mn}^2}{(y_{mn}^2 - m^2)J_m^2(y_{mn})} e^{im(\varphi-\varphi_0)} J_m(y_{mn} r/R) \times J_m(y_{mn} r_0/R)\cos[(2k+1)\pi z/2L]\cos[(2k+1)\pi z_0/2L] \times \exp\left[-\lambda_{mnk}\int_0^t dt' D(t')\right]. \tag{12}$$

The probability that a particle starting from r_0, φ_0, z_0 is not absorbed at time t is given by[20]

$$S(t|r_0, \varphi_0, z_0) = \int_0^{2\pi} d\varphi \int_0^R dr r \int_0^L dz P(r, \varphi, z, t|r_0, \varphi_0, z_0). \tag{13}$$

The function S is, of course, the survival probability, and it can be further simplified to

$$S(t) = \frac{8}{\pi}\sum_{n,k}\frac{(-1)^k}{(2k+1)}\frac{J_1(y_{0n})}{y_{0n}J_0^2(y_{0n})}\exp\left[-\lambda_{0nk}\int_0^t dt' D(t')\right], \tag{14}$$

if one assumes for convenience that $r_0 = z_0 = 0$. (It might seem more realistic to set r_0 to its equilibrium average value, but if the distribution of r_0 in the interval between 0 and R is assumed to be uniform, as is reasonable, one can show that the final results are unchanged from those obtained with the choice $r_0 = 0$.) Both the mean first passage time t_{MFPT} and the distribution of first passage times $f(t)$ can be calculated from $S(t)$, the former using the relation $t_{\text{MFPT}} = \int_0^\infty dt S(t)$ and the latter the relation $f(t) = -\partial S(t)/\partial t$. The evaluation of the derivative of $S(t)$ is trivial, but in order to normalize $f(t)$, the integral $N_1 \equiv \int_0^\infty dt f(t)$ must be evaluated too. This is done by introducing the change of variable $x = \int_0^t dt' D(t')$ into the integral, whereupon N_1 becomes $N_1 = (8/\pi)\sum_{n,k}(-1)^k J_1(y_{0n})/(2k+1)y_{0n}J_0^2(y_{0n})$. Since y_{mn} is the nth zero of $J_{m'}(x)$, and since, in general, $J_{0'}(x) = -J_1(x)$, the zeros of $J_{0'}(x)$ are also the zeros of $J_1(x)$. Now the first zero of $J_1(x)$ is 0, and $J_1(x) = (x/2)(1 - x^2/8 + O(x^4))$ for small x; therefore, all but the first term in the expansion of N_1 over n vanish. Thus, N_1 reduces to $N_1 = (4/\pi)\sum_{k=0}(-1)^k/(2k+1) = 1$. Hence, in

dimensionless variables, we get the *exact* result

$$\frac{f(t)}{(\pi k_B T\tau/mL^2)} = \bar{t}E_{2H,2}[-\bar{t}^{2H}]\sum_{k=0}(-1)^k(2k+1) \times \exp\left[-\left(\frac{(2k+1)\pi}{2}\right)^2\left(\frac{l}{L}\right)^2\bar{t}^2E_{2H,3}[-\bar{t}^{2H}]\right], \tag{15}$$

where the parameters l and $\bar{t}$ have been defined after Eq. (2c).

The evaluation of t_{MFPT} cannot similarly be done exactly, but a closed form expression for this quantity can be obtained in the long time limit $t/\tau \gg 1$, where the asymptotic expansion of the Mittag-Leffler function can be introduced. In this way, one can show that

$$t_{\mathrm{MFPT}} = \frac{\Gamma(q+1)}{\pi}\left(\frac{\zeta L^2\Gamma(2H+1)\Gamma(3-2H)}{4\pi^2k_BT}\right)^q \times\left[\zeta\left(p,\frac{1}{4}\right)-\zeta\left(p,\frac{3}{4}\right)\right], \tag{16}$$

where $q = 1/(2-2H)$, $p = (2-H)/(1-H)$, and $\zeta(a, b)$ is the generalized zeta function, defined as $\zeta(a,b) \equiv \sum_{k=0}^{\infty}(k+b)^{-a}$; it appears by way of the sum $\sum_{k=0}^{\infty}(-1)^k/(2k+1)^p$, which has been evaluated in closed form by MATHEMATICA.[21]

IV. THE INTENSITY CORRELATION FUNCTION

Fluctuations in the fluorescence intensity of labeled transporter proteins passing through single NPCs can also serve as a probe of transmembrane transport. Such fluctuations have been monitored by Hermann *et al.*[7] using near-field scanning optical microscopy (NSOM) (Ref. 22) combined with fluorescence correlation spectroscopy (FCS).[23] In these experiments, the intensity F of the fluorescence emitted by the diffusing particles varies randomly with time (as a result of Brownian motion) and is proportional to the intensity I of the exciting light at a given location. I decays exponentially with distance from the excitation source, which is placed directly above the opening of the NPC. At time t, the deviation $\delta F(t)$ of the emitted intensity from the mean $\langle F(t)\rangle$ is given by $\delta F(t) = F(t) - \langle F(t)\rangle = C_3[I(t) - \langle I(t)\rangle]$, where C_3 is a proportionality constant. The normalized time correlation function $G(t)$ of the emission fluctuation intensity, which is the quantity measured experimentally, is thus given by

$$G(t) = \frac{\langle\delta I(t)\delta I(0)\rangle}{\langle I(0)\rangle^2} = \frac{\langle I(t)I(0)\rangle - \langle I(t)\rangle\langle I(0)\rangle}{\langle I(0)\rangle^2}, \tag{17}$$

where

$$\langle I(t)I(0)\rangle = I_0^2\int_0^R drr\int_0^{2\pi}d\varphi\int_0^L dz\int_0^R dr_0r_0\int_0^{2\pi}d\varphi_0\int_0^L dz_0 \times I(z)P(r,\varphi,z.t|r_0,\varphi_0,z_0)I(z_0)P_{eq}(r_0,\varphi_0,z_0), \tag{18}$$

I_0 is the light intensity at $z = 0$,

$$\langle I(t)\rangle = \langle I(0)\rangle = I_0\int_0^R drr\int_0^{2\pi}d\varphi\int_0^L dzI(z)P_{eq}(r,\varphi,z), \tag{19}$$

with $P_{eq}(r,\varphi,z) = \lim_{t\to\infty}P(r,\varphi,z,t|r_0,\varphi_0,z_0)$, and we have assumed, following Hermann *et al.*,[7] that the emitted light intensity varies only along the axis of the NPC, and that it can be described by the function $I(z) = I_0e^{-z/d}$, d being some characteristic distance.

The probability density function $P(r,\varphi,z.t|r_0,\varphi_0,z_0)$ that is needed in the evaluation of Eq. (18) is obtained from the solution of Eq. (5) under the boundary conditions of Eq. (7) and the initial condition of Eq. (6b). Following the eigenfunction expansion method discussed earlier, we can show that it is given by

$$P(r,\varphi,z,t|r_0,\varphi_0,z_0) = \frac{2}{\pi LR^2}\sum_{mnk}\frac{y_{mn}^2}{(y_{mn}^2-m^2)J_m^2(y_{mn})}e^{im(\varphi-\varphi_0)}J_m(y_{mn}r/R) \times J_m(y_{mn}r_0/R)\cos(k\pi z/L)\cos(k\pi z_0/L) \times\exp\left[-\chi_{mnk}\int_0^t dt'D(t')\right], \tag{20a}$$

where

$$\chi_{mnk} = \left(\frac{y_{mn}}{R}\right)^2+\left(\frac{k\pi}{L}\right)^2. \tag{20b}$$

We can also show from the long time limit of Eq. (20a) that

$$P_{eq}(r,\varphi,z) = \frac{2}{\pi R^2L}. \tag{21}$$

Using these results in Eq. (18), along with standard or tabulated integrals, we find that

$$\langle I(t)I(0)\rangle = \frac{16I_0^2}{L^2}\left[\frac{d^2}{4}(1-e^{-L/d})^2+\sum_{k\neq0}\frac{d^2(1-(-1)^ke^{-L/d})^2}{4(1+d^2k^2\pi^2/L^2)^2} \times\exp\left(-\chi_{01k}\int_0^t dt'D(t')\right)\right]. \tag{22}$$

Similarly, from Eq. (19),

$$\langle I(0)\rangle = \frac{2I_0d}{L}(1-e^{-L/d}). \tag{23}$$

Hence,

$$G(t) = 2\sum_{k=1}^{\infty}\frac{(1-(-1)^ke^{-L/d})^2}{(1+d^2k^2\pi^2/L^2)^2(1-e^{-L/d})^2} \times\exp\left[-k^2\pi^2\frac{k_BT}{mL^2}t^2E_{2H,3}[-(t/\tau)^{2H}]\right], \tag{24}$$

which is the final expression for $G(t)$.

V. DISCUSSION

The key results of this work are the expressions derived above for the mean square displacement [Eq. (2c)], the distribution of mean first passage times [Eq. (15)], the mean first passage time itself [Eq. (16)], and the correlation of intensity fluctuations [Eq. (24)].

Consider first the MSD [Eq. (2c)], which is shown graphically in Fig. 1 as a function of $\bar{t} = t/\tau$ at three different

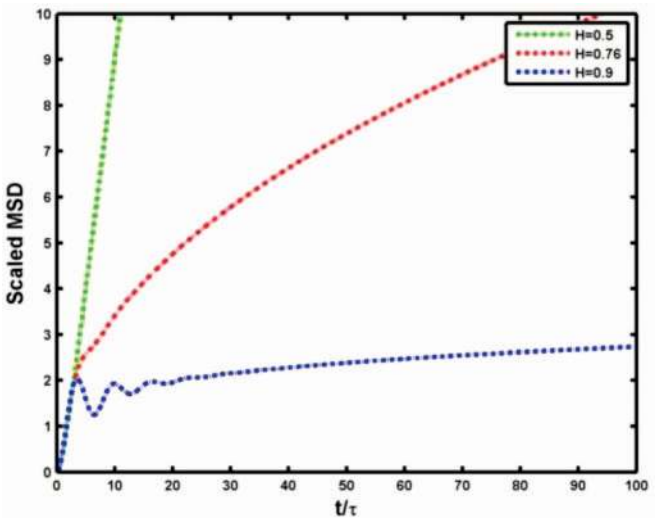

FIG. 1. Variation of the mean square displacement with time (in dimensionless form), as calculated from Eq. (2c) at three different values of the Hurst index H: 0.5 (dashed green line), 0.76 (dashed red line), and 0.9 (dashed blue line).

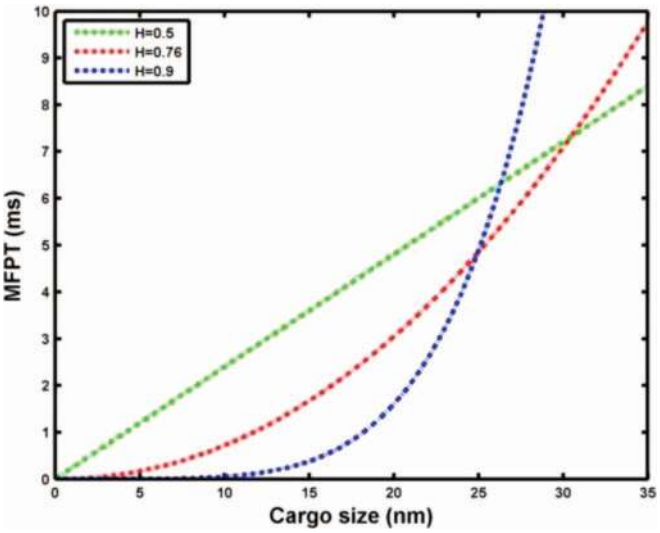

FIG. 2. Variation of the mean first passage time (in ms) with cargo size (in nm), as calculated from Eq. (25), for three different values of H: 0.5 (dashed green line), 0.76 (dashed red line), and 0.9 (dashed blue line). The corresponding b_H values are 0.24 ms nm^{-1}, 5.93 $\times$ 10^{-3} ms nm$^{-2.083}$, and 5 $\times$ 10^{-7} ms nm^{-5}.

values of H (0.5, 0.76, and 0.90). The curves show the progressive effects of increasing the degree of temporal correlation between the thermal forces that drive the particle, with the $H = 1/2$ curve describing simple Brownian motion (uncorrelated forces), and the $H = 0.76$ and $H = 0.9$ curves describing subdiffusive motion (moderately and highly correlated forces, respectively). The curve for $H = 0.9$ bears a close qualitative resemblance to the data obtained in the experiments of Lowe *et al.*[5] (see Fig. 3e of their paper), which tracked protein-functionalized quantum dots (QDs) as they made their way through human NPCs. Ensemble averaged trajectories of the QDs were consistent with a relation of the form $\langle \delta \mathbf{x}^2(t) \rangle \sim t^{\alpha}$, with $\alpha \approx 0.2$ for motion parallel to the pore axis (implying $H = 0.9$; hence, this choice of value in our own analytical expression). The experimental results were interpreted in terms of a scenario involving the "cumulative action of multiple reversible substeps,"[5] essentially the same scenario that underlies both our model and a model introduced recently by Xu *et al.*[24] to explain the subdiffusive behavior of colloidal particles functionalized with "sticky" DNA and allowed to move across a surface coated with the complementary DNA.

When particle motion is subdiffusive, an interesting relation is predicted to exist between the effective hydrodynamic radius of the particle a and the mean first passage time t_{MFPT} to get from one end of the cylinder to the other. In a simple liquid like water, where motion is diffusive, the friction coefficient of the particle ζ varies linearly with a, as dictated by the Stokes equation: $\zeta = 6\pi\eta a$, where η is the viscosity of the medium. If the structure of this relation is assumed to hold even when motion is anomalous, so that ζ continues to vary linearly with a, and η remains, effectively, a measure of viscosity (but now having units that depend explicitly on the Hurst index H), we see from Eq. (16) that

$$t_{MFPT} = b_H a^{1/(2-2H)}, \tag{25}$$

where b_H is a size independent constant. It therefore follows that t_{MFPT} is a linear function of size when motion is diffusive ($H = 1/2$), and a nonlinear function of size when motion is subdiffusive ($H > 1/2$). A plot of t_{MFPT} (in ms) vs a (in nm) is shown in Fig. 2 for the following values of H: 0.50, 0.76 and 0.90. At these respective values of H, the parameter b_H was assigned the values 0.24 ms nm^{-1}, 5.93 $\times$ 10^{-3} ms nm$^{-2.083}$, and 5 $\times$ 10^{-7} ms nm^{-5}, which were chosen for convenience of visual display. (As it happens, when $H = 0.5$, $T = 300$ K, and L is set to the typical pore length of 90 nm, the corresponding value of the viscosity η is 1.30 $\times$ 10^{-2} kg m^{-1}s^{-1}. For a particle of size 10 nm, this translates into a diffusion coefficient D of 1.69 $\times$ 10^{-12} m^{2}s^{-1}, which is a figure typical of small proteins in water. At the slightly larger size of 30 nm, D is 5.63 $\times$ 10^{-13} m^{2}s^{-1}. For the same pore length L, the "viscosities" corresponding to $H = 0.76$ and $H = 0.9$ are, respectively, 0.108 kg m^{-1}s$^{-1.52}$ and 0.220 kg m^{-1}s$^{-1.8}$.) Interestingly, the curve corresponding to $H = 0.9$ reproduces, *qualitatively*, the trends in the variation of t_{MFPT} with a in the simulations of Mincer and Simon[4] (see Fig. 5C of Ref. 4). In these simulations, as well as those of Moussavi-Baygi *et al.*,[3] the relation between t_{MFPT} and a is clearly nonlinear, if not necessarily of exactly the same form as Eq. (25); the relation is distinguished, in particular, by an initial region where t_{MFPT} is relatively insensitive to a followed by a region where t_{MFPT} increases fairly rapidly with a. Up to a certain size threshold, therefore, translocation across the channel can be said to occur fairly quickly; thereafter, it slows down considerably.

Information on the transport mechanism is also contained in the *distribution* of mean first passage times, which in the few experiments and simulations where it has been determined, including those of Kustanovich and Rabin,[25] Lowe *et al.*,[5] and Moussavi-Baygi *et al.*,[6] seems to be distinguished principally by being somewhat broad and asymmetric. Moussavi-Baygi *et al.*[6] have in fact suggested that the distribution can be described by an inverse Gaussian function.

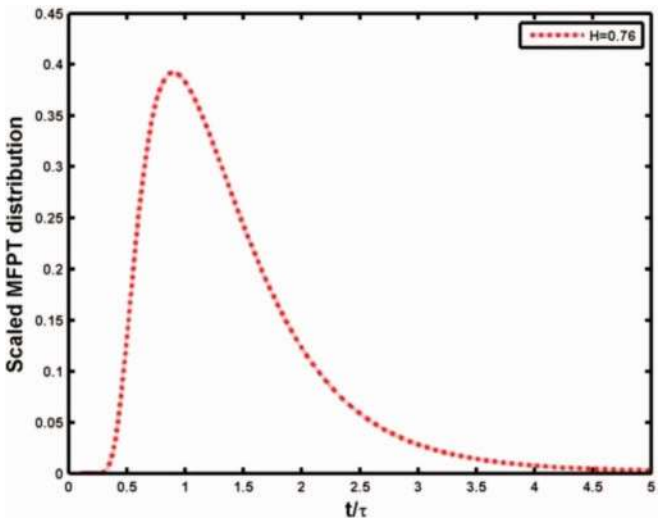

FIG. 3. Time dependence of the first passage time distribution (in dimensionless form) as calculated from Eq. (15), with $H = 0.76$, $l = 71$nm and $\tau = 1$ ms.

This is, of course, quite different from the function obtained in the present calculations [Eq. (15)], which at early times is essentially linear in t, while at late times it is more nearly like a compressed Gaussian. A graph of $f(t)$ [in the dimensionless form given by Eq. (15)] is shown in Fig. 3 at a single representative value of H (0.76) and at the values of $l = 71$nm and $\tau = 1$ms, which were chosen to correspond roughly to the characteristic length and time scales associated with passage through the NPC. The graph is remarkably similar in qualitative appearance to the inverse Gaussian curve that is fit to the simulations of Moussavi-Baygi *et al.*[6] At the other values of H (0.50 and 0.90), and at the same τ but somewhat larger l, the corresponding $f(t)$'s are of almost exactly the same the shape, except for small decreases in height and width of the peak.

The graphs in Figs. 1–3 are meant to illustrate the general patterns of behavior of three different quantities calculated from our model, and to note their broad similarity to the behavior of their experimental or numerical counterparts. We now attempt a somewhat more quantitative comparison of the model's predictions with real data, specifically data from the experiments of Hermann *et al.*[7] on the fluorescence intensity correlations of tagged transporters passing through the NPC. These data correspond to the difference of two sets of experimental measurements, one the intensity correlation function recorded *above* the pore, $G_{above}(t)$, and the other the same function recorded *beside* the pore, $G_{beside}(t)$, the latter being identified with background fluorescence. Hermann *et al.*[7] fit $G_{above}(t) - G_{beside}(t)$ to the following function, obtained from what they refer to as a confined diffusion model (CDM):

$$G_{CDM}(t) = \left[1 + 2\sum_{k=1}^{\infty} \frac{(1-(-1)^k e^{-L/d})^2}{(1+d^2k^2\pi^2/L^2)^2(1-e^{-L/d})^2} \times \exp(-k^2\pi^2 D_0 t/L^2)\right] \exp(-t/T_R). \quad (26)$$

$G_{CDM}(t)$ is identical to the $H = 1/2$ limit of Eq. (24) except for two new terms. (An irrelevant proportionality constant has been omitted in both Eqs. (24) and (26).) The new terms are the factor of unity in front of the summation, and the exponential factor outside the square brackets. We believe the factor of unity is the result of *not* subtracting the term $\langle I(t)\rangle\langle I(0)\rangle = \langle I(0)\rangle^2$ from the term $\langle I(t)I(0)\rangle$ in the expression for the correlation of the intensity fluctuation, $\langle \delta I(t)\delta I(0)\rangle$. This extra factor in turn causes $\langle \delta I(t)\delta I(0)\rangle$ to decay to a *finite* value at $t \to \infty$ rather than to 0, as it should (by construction). The finite long time limit is avoided by introducing, essentially *ad hoc*, the factor of $\exp(-t/T_R)$. Hermann *et al.*[7] justify its inclusion by arguing that it accounts for the kinetics of the binding of the transporter to the pore, a "reaction" assumed to take place on the timescale T_R. T_R is regarded as an adjustable parameter in the theory, and when it is appropriately adjusted, the $G_{CDM}(t)$ fits $G_{above}(t) - G_{besude}(t)$ very well.

However, we believe that $G_{above}(t)$ itself may adequately characterize fluorescence intensity correlations during the entire process of translocation, from binding at the pore to exit from the channel. Under that assumption, our own expression for the correlation function [Eq. (24)] provides a reasonably satisfactory fit to $G_{above}(t)$, as shown in Fig. 4. In this figure, the full black line is the experimental curve corresponding to $G_{above}(t)$, which we have reconstructed[26] from Fig. (6c) of Ref. (7). The dashed red line corresponds to Eq. (24), with H set to 0.76, L set to 90 nm, and d set to 25 nm, the value used in Hermann *et al.*'s calculations, and τ and m set to the best fit values of 1.047×10^{-10}s and 75.54 kDa, respectively. For purposes of comparison, two other curves are shown in Fig. 4: the dashed green line is obtained from Eq. (24) using $H = 0.5$ and the best fit values of $m = 51.5$ kDa, and $\tau = 1.047 \times 10^{-13}$s, all other parameters remaining the

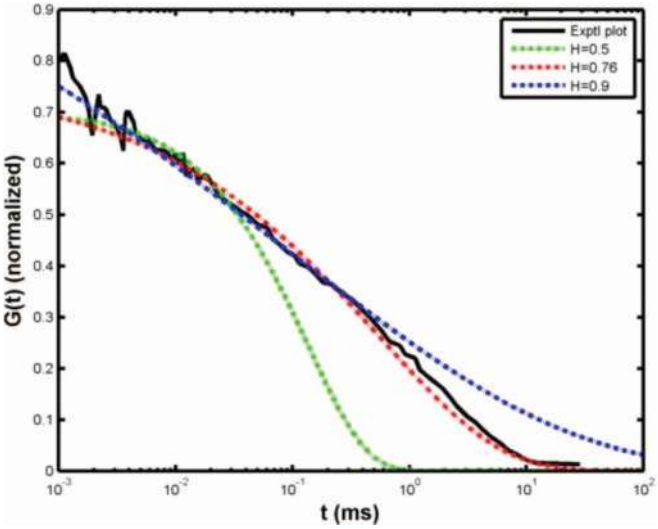

FIG. 4. Dynamic autocorrelation function of fluorescence intensity fluctuations. The full black curve is a reconstruction of the experimental data points in Fig. (6c) of Ref. 7. The colored dashed curves have been calculated from Eq. (24) using different parameter values, as follows: Green ($H = 0.5$, $L = 90$ nm, $d = 25$ nm, $\tau = 1.047 \times 10^{-13}$ s, and $m = 51.5$ kDa); red ($H = 0.76$, $\tau = 1.047 \times 10^{-10}$s, $m = 75.54$ kDa, and L and d remaining the same); and blue ($H = 0.9$, $\tau = 1.047 \times 10^{-9}$ s, $m = 41.27$ kDa, and L and d remaining the same).

same, while the dashed blue is obtained from Eq. (24) using $H = 0.9$ and the best fit values of $m = 41.27$ kDa and $\tau = 1.047 \times 10^{-9}$s, all other parameters remaining the same.

The generally satisfactory agreement between the results of our model and results from various measured or simulated transport properties, as well as the *direct* observation of subdiffusion in the experiments of Lowe *et al.*,[5] seem to suggest that power-law correlations in time between random thermal fluctuations in the medium (the key feature of our model) are involved in the process of facilitated transport through the NPC. Interactions between binding sites on the cargo protein and nucleoporin filaments could potentially produce such power law correlations if their durations spanned a wide range of timescales. That seems to be the case. In the simulations of Moussavi-Baygi *et al.*,[6] for instance, binding interactions were found to last between a few nanoseconds to several microseconds. But in the simulations of Mincer and Simon,[4] on the other hand, the evidence suggests that cargo and filament actually remain bound to each other for the entire duration of the cargo's residence within the NPC—a period on the order of milliseconds—being separated only after action by RanGTPase. Transient interactions of duration intermediate between these extremes are also likely, given that binding affinities span a range of values too, from a few nM to hundreds of nM. It is entirely possible therefore that during translocation, cargo proteins experience different combinations of binding events, some short-lived, some long-lasting, all contributing to the generation of multiple timescales of association.

The above process of stochastic capture and release is also an important element in the models of Kustanovich and Rabin[25] and Zilman *et al.*,[27] to name just two representative examples of early attempts to explain nucelocytoplasmic transport. The first is based on cargo diffusion through a metastable nucleoporin network that can be opened by energetically favorable binding interactions, while the second is based on diffusion through a one-dimensional array of potential wells that represent binding sites. A somewhat different view is expressed in the "reduction of dimensionality" model of Peters,[28] which suggests that cargo proteins bind to nucleoporins principally at the *walls* of the NPC, from where they exit the channel by a two-dimensional (2D) rather than a three-dimensional random walk, achieving generally higher rates of throughput in the process. But the linearity between the mean first passage time and cargo size that is predicted[28] by this mechanism seems to be contradicted by existing data.

The importance of some form of intermittent binding during the course of a transporter's passage through the NPC was also recognized by Licata and Grill,[11] whose analysis of the problem we have adapted. But they too assume, like Peters in the reduced dimensionality approach, that it is principally the walls of the cylinder that are responsible for "stickiness," which they model by an absorbing boundary condition. However, cargo motion itself is not assumed to be restricted to a 2D surface.

Many of the above effects, from subdiffusion to stochastic binding to multiple timescales of association, appear to be at least partly captured by our model through the assumed complex viscoelasticity of the cellular fluid, which is described in terms of a generalized Langevin equation with fractional Gaussian noise. Related models were quite successful in characterizing various aspects of single molecule enzyme kinetics,[29] thermally activated DNA escape from nanopores,[30] fractional viscoelasticity in polymer melts,[31] and the forced unfolding of single polyubiquitin molecules.[32] The present results are therefore broadly consistent with the common mechanisms that seem to underlie a number of seemingly disparate biophysical processes.

[1] R. Y. H. Lim, K. S. Ulman, and B. Fahrenkrog, Int. Rev. Cell Mol. Biol. **267**, 299 (2008); F. Alber, S. Dokudovskaya, L. M. Veenhoff, W. Zhang, J. Kipper, D. Devos, A. Suprapto, O. Karni-Schmidt, R. Williams, B. T. Chait, A. Sali, and M. P. Rout, Nature (London) **450**, 695 (2007); C. Strambio-De-Castillia, M. Niepel, and M. P. Rout, Nat. Rev. Mol. Cell Biol. **11**, 490 (2010); S. R. Wente and M. P. Rout, Cold Spring Harb. Perspect. Biol. **2**, a000562 (2010).

[2] N. Panté and M. Kann, Mol. Biol. Cell **13**, 425 (2002); L. Miao and K. Schulten, Structure **17**, 449 (2009); B. Talcott and M. S. Moore, Trends Cell Biol. **9**, 312 (1999); R. Y. H. Lim, B. Fahrenkorg, J. Köser, K. Schwarz-Herion, J. Deng, and U. Aebi, Science **318**, 640 (2007).

[3] R. Moussavi-Baygi, Y. Jamali, R. Karimi, and M. R. K. Mofrad, Biophys. J. **100**, 1410 (2011).

[4] J. S. Mincer and S. M. Simon, Proc. Natl. Acad. Sci. U.S.A. **108**, E351 (2011).

[5] A. R. Lowe, J. J. Siegel, P. Kalab, M. Siu, K. Weis, and J. T. Liphardt, Nature (London) **467**, 600 (2010).

[6] R. Moussavi-Baygi, Y. Jamali, R. Karimi, and M. R. K. Mofrad, PLoS Comput. Biol. **7**, e1002049 (2011).

[7] M. Herrmann, N. Neuberth, J. Wissler, J. Pérez, D. Gradl, and A. Naber, Nano Lett. **9**, 3330 (2009).

[8] J. Bouchaud and A. Georges, Phys. Rep. **195**, 127 (1990); J. Klafter, M. Shlesinger, and G. Zumofen, Phys. Today **49**(2), 33 (1996).

[9] R. Metzler and J. Klafter, Phys. Rep. **339**, 1 (2000); J. Phys. A.: Math. Gen. **37**, R161 (2004).

[10] J. Ma and W. Yang, Proc. Natl. Acad. Sci. U.S.A. **107**, 7305 (2010); T. Dange, D. Grünwald, A. Grünwald, R. Peters, and U. Kubitscheck, J. Cell. Biol. **183**, 77 (2008); S. Frey, R. P. Richter, and D. Görlich, Science **314**, 815 (2006).

[11] N. A. Licata and S. W. Grill, Eur. Phys. J. E **30**, 439 (2009).

[12] D. Chatterjee and B. J. Cherayil (unpublished).

[13] B. Mandelbrot and J. van Ness, SIAM Rev. **10**, 422 (1968); S. C. Lim and S. V. Muniandy, Phys. Rev. E **66**, 021114 (2002); K. S. Fa and E. K. Lenzi, Phys. Rev. E **71**, 012101 (2005); S. C. Kou, Ann. Appl. Stat. **2**, 501 (2008).

[14] S. Okuyama and D. Oxtoby, J. Chem. Phys. **84**, 5824 (1986); **84**, 5830 (1986).

[15] S. Chaudhury and B. J. Cherayil, J. Phys. Chem. B **112**, 15973 (2008).

[16] D. A. McQuarrie, *Statistical Mechanics* (University Science Books, Sausalito, 2000); R. Zwanzig, *Nonequilibrium Statistical Mechanics* (Oxford University Press, New York, 2001).

[17] A. M. Mathai and H. J. Haubold, *Special Functions for Applied Scientists* (Springer, New York, 2008).

[18] P. Hänggi, in *Stochastic Processes Applied to Physics*, edited by L. Pasquera and M. Rodriguez (World Scientific, Philadelphia, 1985), pp. 69–95; *Noise in Nonlinear Dynamical Systems*, edited by F. Moss and P. V. E. McClintock (Cambridge University Press, New York, 1989), vol. 1, Chap. 9, pp. 307–328; M. San Miguel and M. Sancho, J. Stat. Phys. **22**, 605 (1980); A. Hernández-Machado, J. M. Sancho, M. San Miguel, and L. Pesquera, Z. Phys. B: Cond. Matter **52**, 335 (1983); P. Hänggi, Z. Physik B **31**, 407 (1978).

[19] I. S. Gradshteyn and I. M. Ryzhik, *Table of Integrals, Series and Products* (Academic, San Diego, 1980).

[20] C. W. Gardiner, *Handbook of Stochastic Methods for Physics, Chemistry and the Natural Sciences* (Springer-Verlag, Berlin, 1983).

[21] Wolfram Research, Inc., MATHEMATICA, version 7.0, Champaign, IL, 2008.

[22] A. Lewis, M. Isaacson, A. Harootunian, and A. Muray, Ultramicroscopy **13**, 227 (1984); D. W. Pohl, W. Denk, and M. Lanz, Appl. Phys. Lett. **44**, 651 (1984).

[23] D. Magde, E. L. Elson, and W. W. Webb, Phys. Rev. Lett. **29**, 705 (1972); R. Rigler, U. Mets, J. Widengren, and P. Kask, Eur. Biophys. J. **22**, 169 (1993); O. Krichevsky and G. Bonnet, Rep. Progr. Phys. **65**, 251 (2002).

[24]Q. Xu, L. Feng, R. Sha, N. C. Seeman, and P. M. Chaikin, Phys. Rev. Lett. **106**, 228102 (2011).
[25]T. Kustanovich and Y. Rabin, Biophys. J. **86**, 2008 (2004).
[26]A data digitization program Engauge (downloaded from the web) was used to obtain numerical estimates of the coordinates of the data points.
[27]A. Zilman, S. Di Talia, B. T. Chait, M. P. Rout, and M. O. Magnesco, PLoS Comp. Biol. **3**, e125 (2007).
[28]R. Peters, Traffic **6**, 421 (2005).
[29]S. Chaudhury and B. J. Cherayil, J. Chem. Phys. **125**, 024904 (2006); S. Chaudhury, D. Chatterjee, and B. J. Cherayil, *ibid*. **129**, 075104 (2008).
[30]D. Chatterjee and B. J. Cherayil, J. Chem. Phys. **132**, 025103 (2010).
[31]R. Sharma and B. J. Cherayil, Phys. Rev. E. **81**, 021804 (2010).
[32]D. Chatterjee and B. J. Cherayil, J. Chem. Phys. **134**, 165104 (2011).